MOTION CUE EFFECTS ON HUMAN PILOT DYNAMICS IN MANUAL CONTROL

by

Kyuichiro Washizu*, Keiji Tanaka**,
Shinsuke Endo†, and Toshiyuki Itoko††

*Department of Aeronautics, University of Tokyo, Tokyo, **National Aerospace Laboratory, Tokyo, †The Ministry of Transportation, Osaka, ††Kawasaki Heavy Industry Co., Akashi

ABSTRACT

Two experiments have been conducted to study the motion cue effects on human pilots during tracking tasks. The moving-base simulator of National Aerospace Laboratory was employed as the motion cue device, and the attitude director indicator or the projected visual field was employed as the visual cue device. The chosen controlled elements were second-order unstable systems. It was confirmed that with the aid of motion cues the pilot workload was lessened and consequently the human controllability limits were enlarged. In order to clarify the mechanism of these effects, the describing functions of the human pilots were identified by making use of the spectral and the time domain analyses. The results of these analyses suggest that the sensory system of the motion cues can yield the differential informations of the signal effectively, which coincides with the existing knowledges in the physiological area.

SYMBOLS

B	backward shift operator
c(t)	pilot output
e(t)	error
F_i	shaping filter of forcing function
i(t)	forcing function
K_p	pilot gain
m(t)	output of controlled element
s	Laplace operator
X	damping (rad/sec)
Y	static stability (rad^2/sec^2)
$Y_c(s)$	transfer function of controlled element
$Y_E(s)$	transfer function of human equlizing system
$Y_p(s)$	transfer function of human pilot
$Y_S(s)$	transfer function of human sensory system
Δ	sampling interval (sec)
$\phi_{xy}(j\omega)$	cross power spectrum of x and y
ω	frequency (rad/sec)

INTRODUCTION

There have been several important remarks on the effect of motion cues on the control performance of the human pilot. Through many experimental comparisons between the controls with and without motion, it is well known that the presence of motion generally improves the human control characteristics: it was suggested by Shirley and Young [Ref.1] that the addition of roll-motion cues to the visual ones permitted the pilot to increase his control gain without losing system closed-loop stability; it was also reported by Stapleford et. al. [Ref.2] that the human effective time delay decreased while the lead term of his transfer function increased in the presence of motion cues. Existing human operator models based on these knowledges have been implemented by the results from the studies about the motion sensory organs, especially semicircular canals and otolith [Ref.3].

In this paper we describe two series of experimental studies, both aiming at elucidating differences between the motion and the visual sensor characteristics of the human pilot and correlating them with the physiological knowledges. Both experiments were focused on the critical tracking tasks where the motion cue effects seemed to be dominant. Three experimental conditions, i.e., motion plus visual condition, motion only condition, and visual only condition, were evaluated using the multipurpose research flight simulator of NAL (National Aerospace Laboratory).

THE FIRST EXPERIMENT

Objectives

Purposes of the first experiment are

1) To evaluate the experimental controllability limits of the human pilot controlling second-order unstable systems with and without motion cues, and to confirm the motion cue effects on the controllability limits;

and

2) To investigate the variation of the describing functions of human pilots in controlling unstable systems within their limits by the difference of the kinds of control cues.

Experimental Setup (Fig.1)

In order to close the man-machine feedback loop, subjects were instructed to stabilize the angular motion about the rolling axis, while is similar to the bank angle control of an aircraft, by moving the control stick laterally. An external random forcing function was added into the loop to activate the system. All the signals in the system were recorded by an analogue data recorder to be used later for the identification of the describing functions.

Equipments in Fig.1 are now described:

Controlled element. The transfer function of the controlled element is given by

$$Y_c(s) = \frac{1}{s^2 + Xs + Y} \qquad (1)$$

where Y = 10, 20, 30, 40, 50 (rad^2/sec^2), X < 0, and X was changed with the step size of 0.1 (rad/sec). This unstable second-order controlled element was simulated on an analogue computer.

Control cues. For the input to the pilot in the compensatory tracking task, the error signal in Fig.1 was provided by the following two devices:

(a) *Visual system.* The roll angle was displayed on the attitude director indicator installed in the cockpit.

(b) *Motion system.* A single seated VTOL cockpit was installed on the moving base of the simulator, the maximum operating range of which was ±10 degrees for both sides (Fig.2). The roll axis lay between the subject's feet; his body was subject to both linear and angular accelerations.

Control stick. A single stick-type controller without restoring force was used, generating lateral movements of the control output.

Forcing function. A white noise signal was filtered by the following shaping filter to generate the random forcing function, the power spectrum of which had two gentle cutoff grequencies:

$$F_i(s) = \frac{11}{s^5+5.5s^4+17s^3+28s^2+29s+11} + \frac{1700}{s^4+27s^3+470s^2+3900s+21000} \qquad (2)$$

Two subjects participated in the first experiment; a student who had no experience of controlling aircraft (Pilot A), and a test pilot of NAL (Pilot B). The experimental data were obtained after they had become skilled in the given tracking tasks.

Measurements and Results

Three kinds of experimental situations were realized by changing the cues given to the subject:

(a) *Motion plus visual.* The motion system was drived, and also the instrument information was available.

(b) *Motion only.* Only the motion system was drived, while the room lights were turned off. The subject was requested to close his eyes, and was obliged to utilize motion cues only.

(c) *Visual only.* By fixing the base, only the instrument information was available.

Controllability limits without the forcing function were obtained for Pilot A. The limits were tentatively defined by the parameters X and Y such that the subject could marginally maintain the roll angle within ±10 degrees for one minute. The controllability limits thus obtained are shown in Fig.3. From this figure, it is evident that motion cues have enlarged the limits. This agrees with the existing knowledges concerning the controllability limits and the effectiveness of motion cues.

Next, the describing functions of human pilots were identified by the following procedures. The analogue signals i(t), e(t), c(t) in Fig.1 were converted into digital data with sampling interval $\Delta = 0.05$(sec), with the data length being one minute. On the basis of these ditigal data, the pilot describing functions were obtained as;

$$\hat{Y}_p(j\omega) = \frac{\Phi_{ic}(j\omega)}{\Phi_{ie}(j\omega)} \qquad (3)$$

In Eq.(3) the cross spectra $\Phi_{ie}(j\omega)$, and $\Phi_{ic}(j\omega)$ were computed by Blackman-Tukey method. Correlation functions were cut off to a length of 6(sec), and Hamming window was used. At the same time, the closed-loop linear-correlation coefficient from i(t) to c(t) was calculated as follows:

$$\rho(\omega) = \frac{\Phi_{ic}(j\omega)}{\sqrt{\Phi_{ii}(\omega)\Phi_{cc}(\omega)}} \qquad (4)$$

HITAC 5020 computer was used for the calculation. An example of the obtained results is shown in Figs.4-a and 4-b, of which the values of (X,Y) of

the controlled element correspond to ● in Fig.3. Distinct features easily noticed from the Fig.4-b are summarized as follows:

1) For the case of motion plus visual, gains are generally higher than other cases, and both gains and phases are least fluctuant; i.e., linear-correlation coefficients show high values over wide frequency band. Thus the pilot transfer function of this case seems to be appropriately expressed by;

$$Y_p(s) = K_p \frac{1 + T_L s + T_L s^2}{1 + T_I s} e^{-\tau s} \qquad (5)$$

where $T_L \simeq 0.05$(sec), $T_I \simeq 0.2 \sim 0.5$(sec), respectively.

2) For the case of motion only, the frequency response is similar to that of the case of motion plus visual over the frequency higher than about $1.5 \sim 3$ (rad/sec), where linear-correlation coefficients are large. For the frequency lower than about 1.5(rad/sec), on the other hand, linear-correlation coefficients are small, which implies the irregularity of the control strategy in this frequency band.
3) For the case of visual only, the result is just contrary to the case of motion only, namely, we can see high linear-correlation coefficients in lower frequency band; while in higher frequency band the response are dispersed and linear-correlation coefficients are small.
4) The increase of gains, which is obvious in higher frequency band of both motion cases, corresponds to the rather rapid control stick movements observed in Fig.4-a. This phenomenon can be seen often in tracking when a controlled element is oscillatory. In such a case, human pilot seems to obtain quickness, which is especially important for the system stability, by oscillating the stick with the frequency that is suited to him and is higher than the natural frequency of the controlled element.

The features listed above are consistently observed regardless of subjects or controlled elements. Thus, it was confirmed that motion cues improved the human control characteristics in high frequency range which was important for the system stability, and that visual cues given by the instrument were effective to the precise control in rather low frequency range; i.e. visual cues bring about such an improvement of control as cancelling the steady-state deviations.

THE SECOND EXPERIMENT

In the first experiment, the control for the case of visual only corresponds to the flight in the instrument meteorological condition (IMC) without motion cues. On the other hand, in the case of motion plus visual, subjects could use not only instrument information but also the peripheral visual information; namely the situation is equivalent to the flight in the visual meteorological condition (VMC) with motion cues. Consequently there was the difference of visual information between the above two conditions. The recent paper by Junker et. al. [Ref.4] also points out that the peripheral visual information has the same effect on the human pilot control strategy as motion cues.

The second experiment was resumed after modifying the visual system so as to equalize the visual information for the cases of visual only to motion plus visual only: the visual information was provided by the simulated visual field projected to the screen in front of the cockpit to widen the pilots' angle of vision. Moreover, to put a stress on the study of the describing functions, slightly unstable controlled elements were adopted. In addition, the time domain analysis, which has recently come into practical use, has revealed the possibility of identifying precisely both system dynamics and noise characteristics. We have employed this technique in order to investigate the human sensory characteristics.

Thus the second experiment has the following two objectives:
1) To get the differences between pilot dynamics with and without motion cues by providing the pilot with the visual cues similar to those of VMC; and
2) To estimate the mechanism of the motion and the visual sensory organs, based on the describing functions and the remnants.

Experimental Setup

Only the modifications of the first experiment are described. The block diagram was the same as Fig.1.

Controlled element.

$$Y_c(s) = \frac{Y}{s^2 + Xs + Y} \qquad (8)$$

Static gain was set constant, and the parameters were $Y = 10$, 30 and $X = 0$, -0.3, respectively.

Cockpit and controller. Both were the same as those of the first experiment.

Control cues.

(a) *Visual system*: Simulated visual field was used, which was the scene of the scaled runway taken by a video camera, and was projected on the wall screen in front of the cockpit by Eidophor (Fig.5). The pilot visual angle was widened to 32 degrees laterally by these equipment. For the case of motion plus visual the image was fixed, while for the case of visual only it was rotated to provide pilots with the visual information of rolling, by coordinatedly rotating the video camera.
(b) *Motion system*: The same cockpit was used.

Forcing function. The random signal of limited band-width was utilized, the shaping filter of which was simplified to;

$$F_i(s) = K\left[\frac{10}{(1+s)^2} - \frac{1}{(1+0.1s)^2}\right] \qquad (7)$$

Measurement and Analysis

The subject participated in the second experiment was Pilot B of the first experiment. After having got fully accustomed to the system, he conducted about 30 runs which could be classified by the combination of the control cues provided as;

1) *Motion plus visual.* The simulated visual field was fixed, and the motion base was derived.
2) *Motion only.* The motion base was drived. The subject was requested to close his eyes, with the room lights extinguished.
3) *Visual only.* The motion base was fixed. The simulated visual field was rotated to provide visual cues as if the cockpit were rotating.

The obtained data were processed in the same manner as in the first experiment, except that the sampling interval was changed to $\Delta = 0.1$(sec). Pilot describing functions were identified according to the following two ways by making use of FACOM 230-75 computer.

1) *Cross-power spectrum method.* This is the same method as that of the first experiment, and was applied by setting the correlation length to 10 (sec) and using Hamming window.
2) *MFPE (Multiple Final Prediction Error) method.* An autoregressive model is fitted to the data by using Akaike's MFPE method [Refs.5,6]. This model can be expressed as;

$$\begin{bmatrix} c(n) \\ e(n) \end{bmatrix} = \begin{bmatrix} A_{11}(B) & A_{12}(B) \\ A_{21}(B) & A_{22}(B) \end{bmatrix} \begin{bmatrix} c(n) \\ e(n) \end{bmatrix} + \begin{bmatrix} \sigma_{11} & 0 \\ 0 & \sigma_{22} \end{bmatrix} \begin{bmatrix} \xi_1(n) \\ \xi_2(n) \end{bmatrix} \qquad (8)$$

where c(n) and e(n) are sampled time series obtained from c(t) and e(t) with the sampling interval Δ, and

$$A_{ij}(B) = a_{ij}(1)B + a_{ij}(2)B^2 + \cdots\cdots + a_{ij}(M)B^M \qquad (i,j=1,2),$$

where B is backward shift operator; i.e., $Bx(n) = x(n-1)$, and $\xi_1(n)$, $\xi_2(n)$ are mutually independent white noises. From Eq.(8), we can derive a pilot describing function as:

$$\hat{Y}_p(j\omega) = \frac{A_{12}(j\omega)}{1 - A_{11}(j\omega)} \qquad (9)$$

where $A_{11}(j\omega)$, $A_{12}(j\omega)$ are obtained from $A_{11}(B)$, $A_{12}(B)$ by substituting $e^{-j\omega\Delta}$ for B.

The describing functions obtained by both methods are in good accordance with each other. An example of the describing functions obtained by the latter method is shown in Fig.6. The controlled element of this example corresponds to ⑧ in Fig.3. The characteristics shown in Fig.6 generally coincide with those of the first experiment, i.e., when motion cues are available, high control gains are observed.

Discussions

In the following, we consider a human pilot model which consists of the sensory part, Y_S, and the equalizing and neuro-muscular part, Y_E, corresponding to the forward and the afterward part of the human describing function with respect to the injection point of the remnant source, w(t) [Fig.7] In Fig.7, w(t) corresponds to $\sigma_{11}\xi_1(n)$ of Eq.(8), and assumed to be white. On the basis of this model, the estimates of the two parts, $\hat{Y}_S$ and $\hat{Y}_E$ were calculated. Refering to Appendix, we obtain the following relations;

$$\hat{Y}_S(j\omega) = A_{12}(j\omega) \qquad (10)$$

and

$$\hat{Y}_E(j\omega) = \frac{1}{1 - A_{11}(j\omega)} \qquad (11)$$

Examples of $\hat{Y}_S$ and $\hat{Y}_E$ thus obtained are shown in Figs.8 and 9. These figures show that Y_S's with motion indicate high gain and differential or second-order differential features, while Y_E's with motion remain generally the same. The estimated magnitudes of the remnant source of these cases have proved to differ depending on the provided cues by no more than 2db, which can be considered to be almost equal to one another. This suggests the validity of the above partition of the human describing function.

For further examinations of the differences in Y_S's, we should consider the remnant sources. It has been suggested that the remnant can be attributed to the following sources [Refs.7,8].

(a) *Modelling errors.* We often express the pilot dynamics as the continuous linear time-invariant system, but the human control strategy practically contains discrete, nonlinear and time-varing features, which are lumped together as the remnant when we construct a model.
(b) *The response to the signals other than the input.*
(c) *Noises that the human pilot generates by himself.* These are classified into the observation noise which is injected at the sensory system, noise during the processings in his celebrum, and the motor noise in the neuro-muscular system.

Among them, (a) and (b) are considered to be small when the subject is well trained and highly motivated, and when the task is a simple single-axis tracking. Moreover, among (c), the motor noise is usually regarded insignificant. Thus it seems proper to consider that the remnant sources of this case are injected at the sensory system or near celebrum. This leads to us to attribute the causes of the differences in Y_S's to the differences of the sensory

system. This therefore implies that the differential or the second-order differential features in Y_S's in motion cases reflect the dynamics of the motion sensor organs. We can see that motion cues could be effectively utilized with a low level remnant. On the other hand, pilot dynamics based on the visual cues proved to have smaller gain and the visual cues are more insensitive than the motion cues.

Although an assumption concerning the remnant source puts some restrictions on the previous discussion, the findings mentioned above basically agr with the physiological knowledges about the vestibular organs. It should be noted that the sensor organs investigated in this experiment are equivalent to the integrated motion sensor system including not only the vestibular organs but also the skin sensations and the deep sensations. To make the obtained results more practical, we should continue further evaluation of these findings by carefully comparing these with the knowledges about the human sensor dynamics.

CONCLUDING REMARKS

From the experiments described above, we conclude as follows:

1) Motion cues can enlarge the human pilots' controllability limits for the second-order unstable controlled elements.
2) Motion cues improve the human control characteristics in rather high frequency range, while the visual cues are effective for the precise control in rather low frequency.
3) From the discussions about human describing functions and the remnant, it was suggested that the motion sensor system can yield the differential or the second-order differential informations of the input.

ACKNOWLEDGEMENT

The authors are deeply indebted to Mr. Y. Terui, a test pilot of NAL, for his participation as the subject, and also to Prof. N. Goto of Kyushu University for his comments on this paper.

REFERENCES

1. Shirley,R.S.; and Young,L.R.: Motion Cues in Man-Vehicle Control. IEEE Trans., Vol.MMS-9, 1968.

2. Stapleford,R.L.; Peters,R.A.; and Alex,F.R.: Experiments and a Model for Pilot Dynamics with Visual and Motion Inputs. NASA CR-1325, 1969.

3. Curry,R.E.; Young,L.R.; Hoffman,W.C.,; and Kugel,D.L.: A Pilot Model with Visual and Motion Cues. Proc. of AIAA Visual and Motion Simulation Conference, 1976, pp.50-54.

4. Junker,A.M.; and Price,D.: Comparison between a Peripheral Display and Motion Information on Human Tracking about the Roll Axis. Proc. of AIAA Visual and Motion Simulation Conference, 1976, pp.63-72.

5. Tanaka,K.; Goto,N.; and Washizu,K.: A Comparison of Techniques for Identifying Human Operator Dynamics Utilizing Time Series Analysis. 12th Ann. Conf. on Manual Control, NASA TM X-73,170, 1976, pp.673-685.

6. Akaike,H.: Autoregressive Model Fitting for Control. Ann. Inst. Statist. Math., Vol.23, 1971, pp.163-180.

7. McRuer,D.T.; and Krendel,E.S.: Mathematical Models of Human Pilot Behavior. AGARD-AG-188, 1974.

8. Levison,W.H.; and Kleinman,D.L.: A Model for Human Controller Remnant. 4th Ann. Conf. on Manual Control, NASA SP-192, 1968, pp.3-14.

APPENDIX: ON THE SHAPING FILTER OF THE HUMAN REMNANT

We generally define the remnant r(t) as a portion of c(t) irrelevant to e(t); namely

$$r(t) = c(t) - \int_0^t y_p(t-\tau)e(\tau)d\tau \qquad \text{I}$$

where $y_p(\tau)$ is the weighting function of $Y_p(j\omega)$. From Fig.7, we can derive the following relation:

$$c(t) = \int_0^t y_p(t-\tau)e(\tau)d\tau + \int_0^t y_E(t-\tau)w(\tau)d\tau \quad , \qquad \text{II}$$

where $y_E(\tau)$ is the weighting function of $Y_E(j\omega)$. From Eq.I and II, r(t) is considered to be a shaped output of Y_E activated by the white noise w(t); therefore the shaping filter of r(t) is Y_E. Thus we have Y_S as;

$$Y_S(j\omega) = \frac{Y_p(j\omega)}{Y_E(j\omega)} \quad . \qquad \text{III}$$

We shall begin here by introducing the way to get Y_E by making use of the spectral method. It is well known that the coherency between i(t) and c(t) is

$$\rho^2(\omega) = \frac{|\Phi_{ic}(j\omega)|^2}{\Phi_{ii}(\omega)\Phi_{cc}(\omega)} \quad . \qquad \text{IV}$$

If we denote the power spectrum of closed-loop contribution of the remnant as

$$\Phi_{pp}(\omega) = \left|\frac{1}{1 + Y_p(j\omega)Y_c(j\omega)}\right|^2 \Phi_{rr}(\omega) \qquad \text{V}$$

where

$$\frac{1}{1 + Y_p(j\omega)Y_c(j\omega)} = \frac{\Phi_{ie}(j\omega)}{\Phi_{ii}(\omega)} \quad ,$$

we can write

$$\Phi_{pp}(\omega) = \{1 - \rho^2(\omega)\}\Phi_{cc}(\omega) \qquad \text{VI}$$

From Eqs.V and VI, we obtain the estimat of the power spectrum of the remnant by;

$$\Phi_{rr}(\omega) = \frac{\Phi_{ii}^2(\omega)\Phi_{cc}(\omega) - \Phi_{ii}(\omega)|\Phi_{ie}(j\omega)|^2}{|\Phi_{ie}(j\omega)|^2} \qquad \text{VII}$$

While

$$\Phi_{rr}(\omega) = |Y_E(j\omega)|^2 W \quad , \qquad \text{VIII}$$

where W denotes the intensity of w(t). Thus we can estimate $|Y_E(j\omega)|$ from VII and VIII, by the spectral method.

Next, we introduce another way to obtain Y_E from the autoregressive model defined in the time domain. We shall rewrite the first equation of Eq.(8) as;

$$c(n) = A_{11}(B)c(n) + A_{12}(B)e(n) + \sigma_{11}\xi_1(n) \quad , \qquad \text{IX}$$

where

$$w(n) = \sigma_{11}\xi_1(n) \quad .$$

Arranging IX, we obtain

$$c(n) = \frac{A_{12}(B)}{1 - A_{11}(B)} + \frac{\sigma_{11}}{1 - A_{11}(B)}\xi_1(n) \quad , \qquad \text{X}$$

where the second term of the right hand side corresponds to the open-loop contribution of w(t) to c(t); namely

$$r(n) = \frac{\sigma_{11}}{1 - A_{11}(B)}\xi_1(n) \quad . \qquad \text{XI}$$

Therefore we obtain the shaping filter of r(t) by Fourier-transforming $\{1 - A_{11}(B)\}^{-1}$ as;

$$\hat{Y}_E(j\omega) = \frac{1}{1 - A_{11}(j\omega)} \quad , \qquad \text{XII}$$

While the human describing function is,

$$\hat{Y}_p(j\omega) = \frac{A_{12}(j\omega)}{1 - A_{11}(j\omega)} \quad . \qquad \text{XIII}$$

Thus, we can easily estimate Y_S by,

$$\hat{Y}_S(j\omega) = A_{12}(j\omega) \quad . \qquad \text{XIV}$$

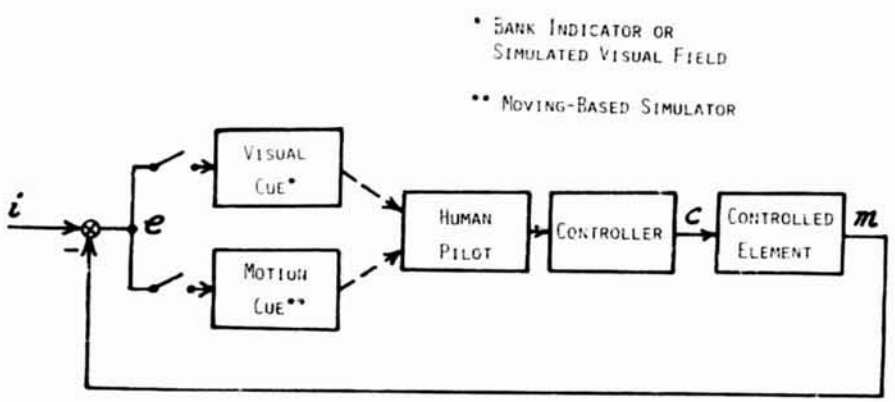

Figure 1. Block Diagram of the Experiments

Figure 2. NAL VTOL Cockpit

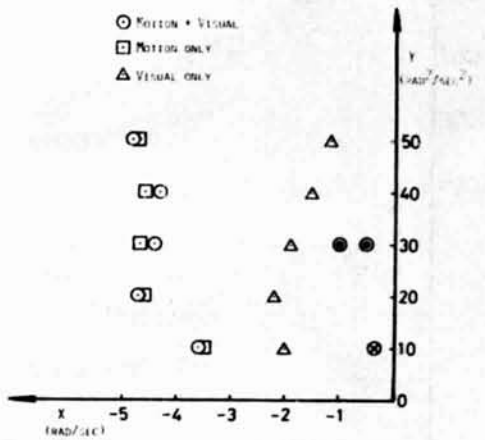

Figure 3. Controllability Limits for Unstable Second-Order Controlled Elements

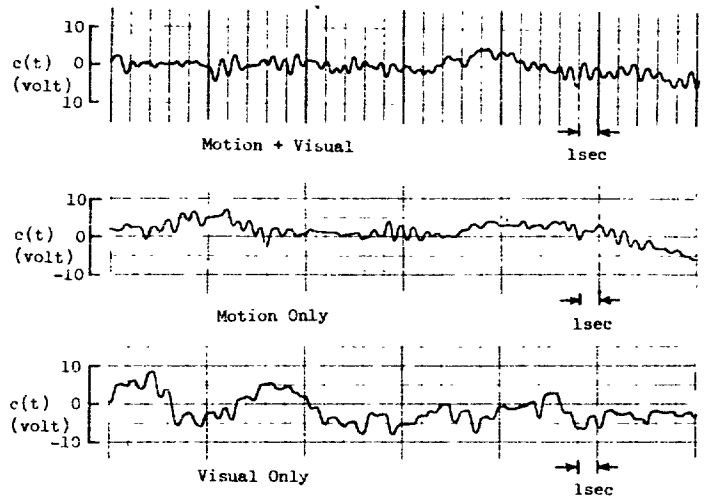

Figure 4-a. Typical Control Deflections

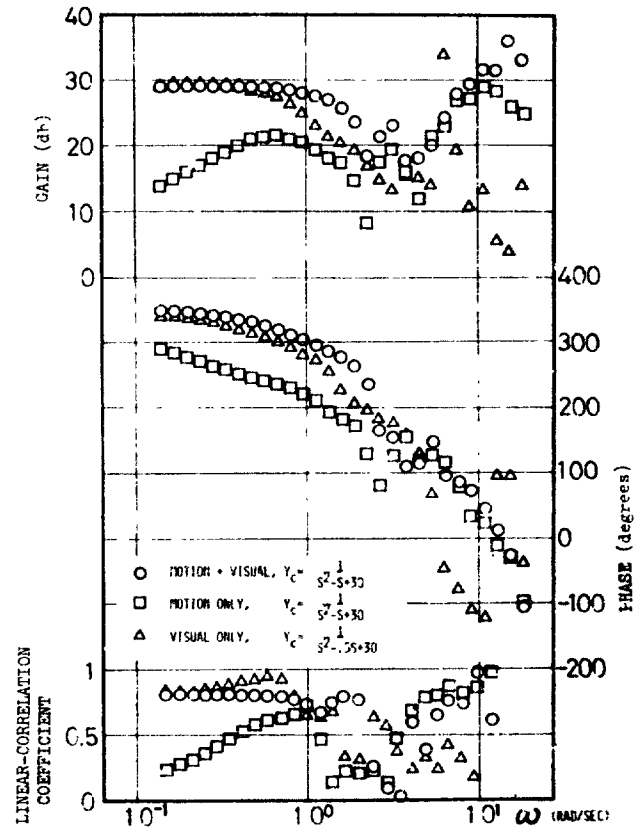

Figure 4-b. Identified Pilot Describing Functions, $\hat{Y}_p(j\omega)$'s by Spectral Method

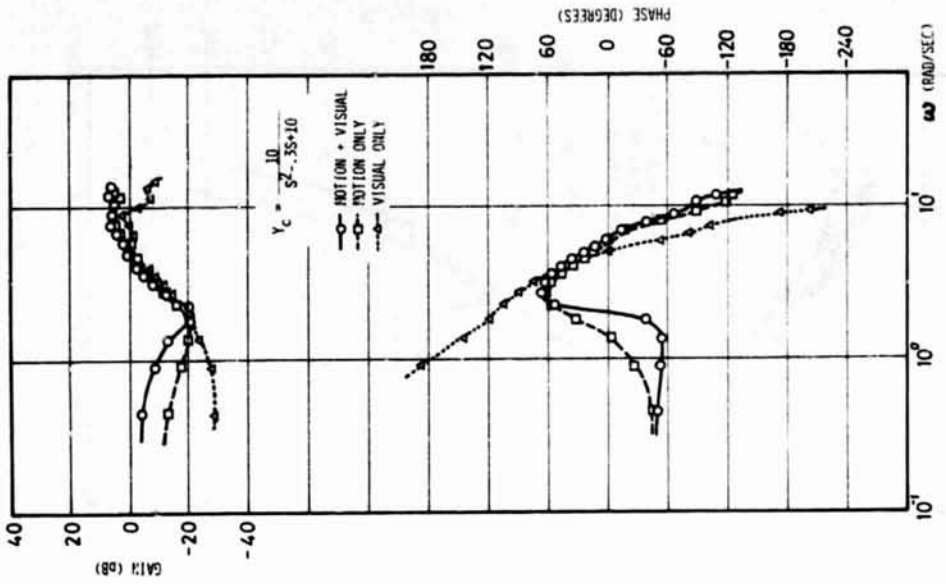

Figure 6. $\hat{Y}_p(j\omega)$ by MFPE Method

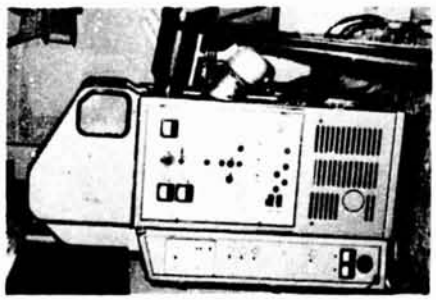

Figure 5-a. Video Projector (Eidophor)

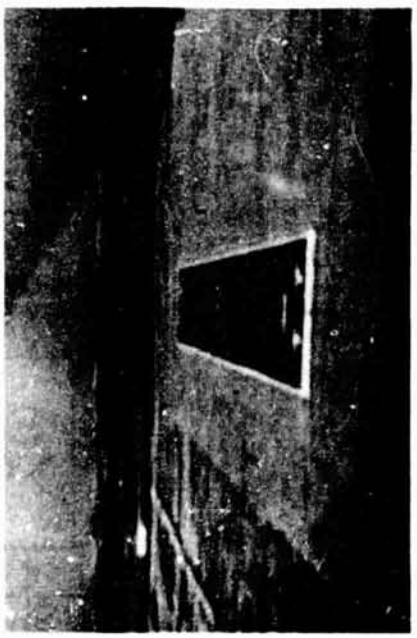

Figure 5-b. Simulated Visual Field

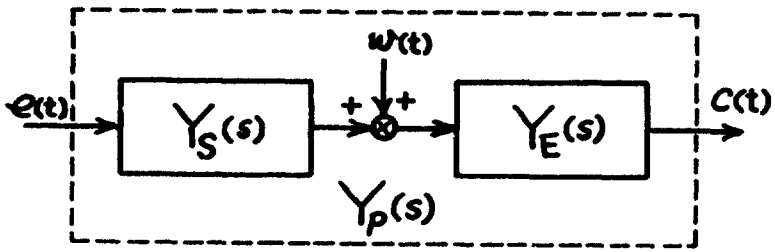

Figure 7.- Partition of $Y_p(s)$

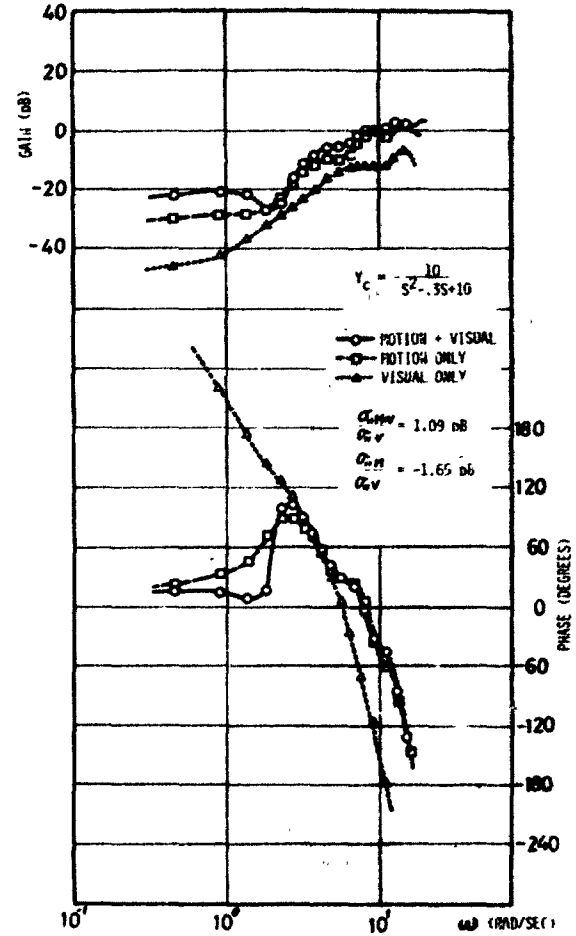

Figure 8. $Y_S(j\omega)$

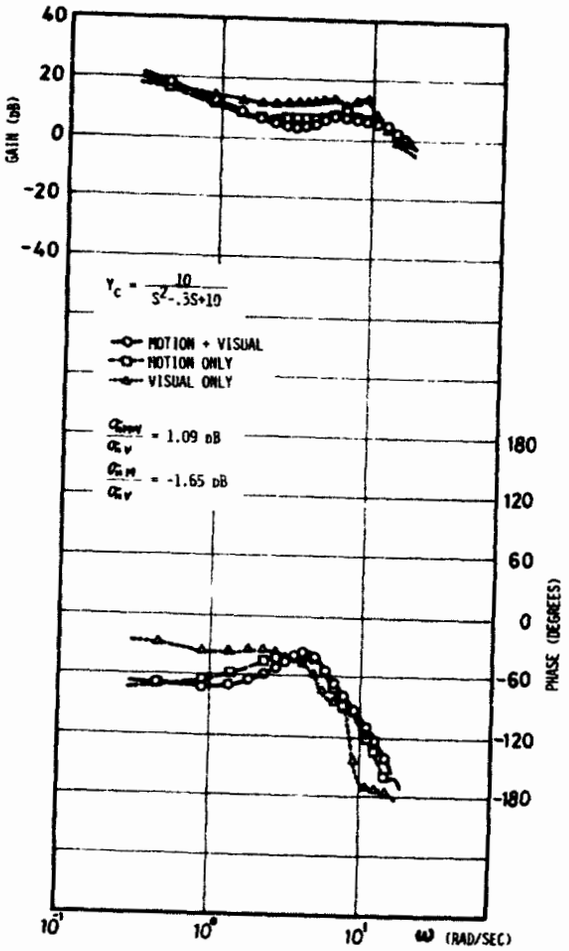

Figure 9. $\hat{Y}_p(j\omega)$